

Self-Assembled ABC Triblock Copolymer Double and Triple Helices**

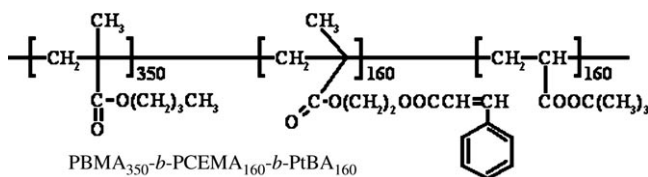
John Dupont, Guojun Liu,* Ken-ichi Niihara, Ryuhei Kimoto, and Hiroshi Jinnai

In a block-selective solvent, the insoluble block or blocks of a block copolymer agglomerate to form nanometer-sized micelle-like aggregates, which are stabilized against further agglomeration by the soluble block(s). Depending on the composition of the copolymer, the interfacial tension between the solvent and the insoluble block(s), and other factors, the shape of the aggregates formed can be spherical,^[1] vesicular,^[2–5] tubular,^[6–8] cylindrical,^[9–15] etc. The shape diversity of such aggregates facilitates their applications in nanofabrication, lithography, cell culturing, and drug delivery.

Most of the previous solution self-assembly studies of block copolymers were performed for AB diblock copolymers. The natural choices for solvents have been block-selective solvents, which solubilize one block of an AB diblock copolymer, but not the other. With ABC triblock copolymers, the solvent choice becomes much more interesting. Traditionally, solvents selective for one terminal block (A or C) or for two consecutive blocks (A and B or B and C) were used.^[16,17] With rare exceptions,^[13,14,18–22] the use of such solvents led to core-shell-corona spherical or cylindrical aggregates. More recently, solvents selective for the A and C terminal blocks have been used, and the use of such solvents has led to aggregates with interesting coronal-chain segregation patterns.^[8,23,24] We report in this paper the self-assembly of an ABC triblock copolymer in solvents that are good for C, poor for B, and marginal for A. We report also our surprising discovery that, after a long period of sample ageing, the self-assembled aggregates were double and sometimes triple helices. Even more surprising, such structures were formed in three different solvent systems that we have tested so far.

The triblock copolymer used was poly(*n*-butyl methacrylate)-*block*-poly(2-cinnamoyloxyethyl methacrylate)-*block*-poly(*tert*-butyl acrylate) or PBMA₃₅₀-*b*-PCEMA₁₆₀-*b*-

PtBA₁₆₀ consisting of 350 BMA units, 160 CEMA units, and 160 tBA units. The precursor to this polymer was prepared by anionic polymerization and had a low polydispersity index of 1.06 (see the Supporting Information).



The marginal solvent mixtures were prepared from dichloromethane and methanol, tetrahydrofuran (C₄H₈O) and methanol, and chloroform and methanol. Relying on the solubility behavior of model homopolymers PtBA₁₀₅, PCEMA₁₉₅, and PBMA₄₆₀, we established that CH₂Cl₂, C₄H₈O, and CHCl₃ were good solvents for all the three blocks of the copolymer. Methanol was poor for PBMA and PCEMA but good for PtBA. Furthermore, PCEMA₁₉₅ became insoluble when the methanol volume fraction f_M was higher than $(46.0 \pm 2.5)\%$ in CH₂Cl₂/CH₃OH and $(49.0 \pm 2.5)\%$ in C₄H₈O/CH₃OH or CHCl₃/CH₃OH. The critical f_M values for PBMA₄₆₀ precipitation were $(85.0 \pm 2.5)\%$ in CH₂Cl₂/CH₃OH or CHCl₃/CH₃OH and $(80.0 \pm 2.5)\%$ in C₄H₈O/CH₃OH. Thus, we used CH₂Cl₂/CH₃OH with $f_M = 82\%$, C₄H₈O/CH₃OH with $f_M = 77\%$, and CHCl₃/CH₃OH with $f_M = 83\%$ as the marginal mixtures for PBMA for the self-assembly of the triblock copolymer.

Aggregate preparation was performed by first dissolving the polymer in CH₂Cl₂, C₄H₈O, or CHCl₃ and then adding CH₃OH over a period of 1 min until the desired f_M value was reached. At this stage, our transmission electron microscopy (TEM) analyses indicated that the triblock copolymer formed mostly spherical aggregates. Our NMR analysis suggested that the PtBA and PBMA chains were not segregated but were well mixed in the corona of the spherical aggregates (see the Supporting Information).

Our suspicion was that the spherical aggregates were formed at $f_M \approx 50\%$, when PCEMA first segregated out from the solvent phase. Although spherical aggregates were probably the favored products at $f_M \approx 50\%$, the situation changed in CH₂Cl₂/CH₃OH with $f_M = 82\%$, in CHCl₃/CH₃OH with $f_M = 83\%$, or in C₄H₈O/CH₃OH with $f_M = 77\%$ when the PBMA chains became marginally soluble and much more compact. If the PBMA chains are viewed, in terms of the classical geometric-packing parameter theory,^[25] as the “heads” of a micelle (the heads are normally solvated and, in this case, the PBMA block is marginally soluble), much less

[*] J. Dupont, Prof. G. Liu
Department of Chemistry
Queen's University
90 Bader Lane, Kingston, Ontario, K7N 3N6 (Canada)
Fax: (+1) 613-533-6996
E-mail: guojun.liu@chem.queensu.ca
Homepage: <http://www.chem.queensu.ca/people/faculty/Liu/index.htm>

Dr. K.-i. Niihara, R. Kimoto, Prof. H. Jinnai
Department of Macromolecular Science & Engineering
Kyoto Institute of Technology
Matsugasaki, Kyoto 606-8585 (Japan)

[**] G.L. thanks the NSERC of Canada for sponsoring this research. H.J. thanks the Ministry of Education, Science, Sports and Culture for support through Grants-in-aid 19031016, 21015017, and 21241030.

Supporting Information for this article is available on the WWW under <http://dx.doi.org/10.1002/anie.200901517>.

surface area should be required to accommodate the PBMA chains at these solvent compositions than at $f_M = 50\%$. Thus, we anticipated a morphological transition from spherical aggregates to cylindrical or vesicular aggregates for the copolymer under these solvation conditions.

We followed the structural evolution of the aggregates in $\text{CH}_2\text{Cl}_2/\text{CH}_3\text{OH}$ at $f_M = 82\%$ by taking samples for TEM analysis at different sample-aging times. Figure 1 shows TEM

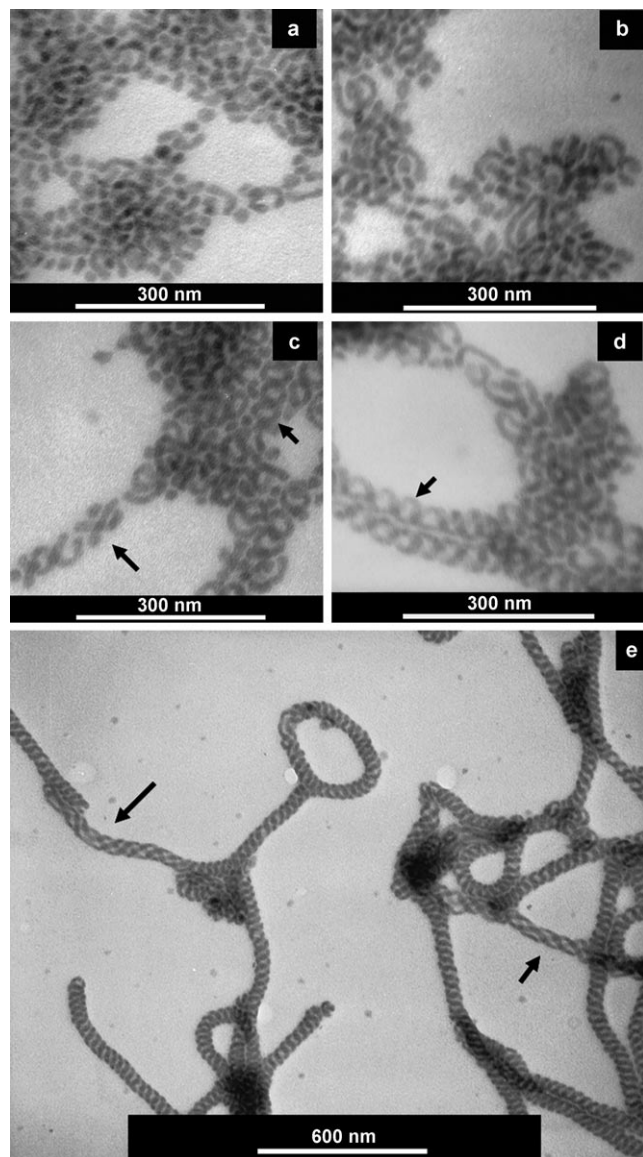


Figure 1. TEM images of aggregates sprayed from $\text{CH}_2\text{Cl}_2/\text{CH}_3\text{OH}$ at $f_M = 82\%$ after sample aging for a) 1, b) 8, c) 16, d) 24, and e) 90 d. The samples were stained by OsO_4 .

images of such samples sprayed onto carbon-coated copper grids and stained by the PCMA-selective OsO_4 . Only the PCMA domains should be visible.

After 1 day of sample aging, cylindrical aggregates were observed, together with spherical aggregates (Figure 1a). After 8 days, the cylinders were longer (Figure 1b). Also, the long cylinders were mostly curved. After 16 days, many of the

curved cylinders started to form crosses (one marked by a long arrow in Figure 1c) and seemed to be positioned for fusion into helices. Some formed helical sections were also seen (one marked by a short arrow in Figure 1c). After 24 days, long double helices were observed (marked by an arrow in Figure 1d). After 3 months, helices with periodic pitches were observed (Figure 1e).

The results of this kinetic experiment suggest that the helices were probably the equilibrium aggregates or micelles in $\text{CH}_2\text{Cl}_2/\text{CH}_3\text{OH}$ at $f_M = 82\%$. Also, the helices seemed to have formed from a fusion mechanism, which involved the fusion of spheres into cylinders, the crossing of the cylinders, and then the stacking and fusion of cylinders into helices. The fact that the different cylinders formed crosses and the different crosses stacked together suggests that the marginally solubilized coronal PBMA chains of different cylinders attracted one another and functioned as glue between the different nanoobjects.

Most of the helices after 3 months appear to be double helices. Occasionally, triple helices (two marked by arrows in Figure 1e) were seen. Conventional TEM gives the projection of a 3D structure at one sample-tilting angle. Structural deduction based on such images can lead to erroneous conclusions. We have also performed TEM tomography analysis of a helix sample prepared in $\text{CH}_2\text{Cl}_2/\text{CH}_3\text{OH}$ at $f_M = 82\%$. Such an analysis involved taking projections of the helices at sample-tilting angles between -71° and 77° at 1° intervals and then reconstructing a 3D image from all of the projections with a computer. Figure 2 shows the 3D images of

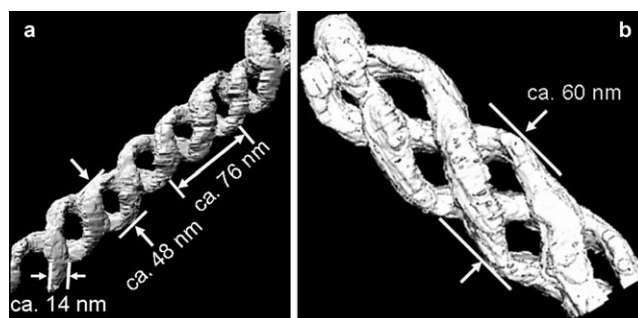


Figure 2. TEM tomography images of a) double and b) triple helices sprayed from $\text{CH}_2\text{Cl}_2/\text{CH}_3\text{OH}$ at $f_M = 82\%$.

a left-handed double helix and a right-handed triple helix, which verifies the structures unambiguously. Overall, the double and triple helices had no preferred twisting sense because the block copolymer used had no chirality.

As marked in Figure 2a, the pitch length of the double helix was approximately 76 nm. Our analysis also indicated that the cross-section of the PCMA strands was not circular but elliptical. The transverse diameter of such an ellipse was approximately 14 nm and the conjugate diameter was about 7 nm. Furthermore, the double helix was flattened on the TEM grid surface. The height spanned by the PCMA strands was approximately 19 nm and the width was about 48 nm. The triple helices were somewhat wider than the

double helices. The width spanned by the triple PCEMA strands was approximately 60 nm (Figure 2b).

Multiple helices were also formed in $\text{C}_4\text{H}_8\text{O}/\text{CH}_3\text{OH}$ at $f_{\text{M}} = 77\%$ and in $\text{CHCl}_3/\text{CH}_3\text{OH}$ at $f_{\text{M}} = 83\%$. Figure 3 shows

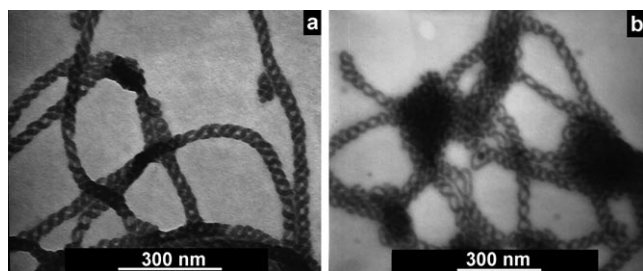


Figure 3. TEM images of helices sprayed from a) $\text{C}_4\text{H}_8\text{O}/\text{CH}_3\text{OH}$ at $f_{\text{M}} = 77\%$ and b) $\text{CHCl}_3/\text{CH}_3\text{OH}$ at $f_{\text{M}} = 83\%$. The samples were stained by OsO_4 .

TEM images of helices sprayed from these two solvent mixtures and stained by OsO_4 . The helices were prepared by aging the samples for 3 weeks. Evidently, the helical structure was better developed in $\text{C}_4\text{H}_8\text{O}/\text{CH}_3\text{OH}$, probably because of the lower methanol content used and, thus, the higher mobility of the PCEMA core chains in this case.

Figure 4a depicts the structure, based on our understanding so far, of a section of a double helix. The PCEMA core of

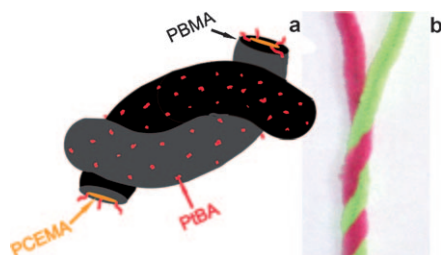


Figure 4. a) Schematic representation of the chain packing in a double-helix section. b) Photograph of two pipe cleaners twisted into a double helix.

each helix strand has an elliptical cross-section. We do not know exactly how the PtBA and PBMA chains are distributed in the corona. We suspect that more PtBA chains are packed on the surface exposed to the solvent to provide better steric stabilization to the double helices. The PBMA chains are concentrated on the contacting side to improve the mixing of the PBMA chains of the different strands. Indirect evidence supporting this hypothesis was that most of the cylinders were bent rather than straight even before helix formation. The bending probably occurred due to an asymmetric coronal-chain distribution.

The reproducible formation of multiple helices from this triblock copolymer in three solvent pairs under marginal solubilization conditions for PBMA suggests that the helices were thermodynamic products. Although cylinder formation is not surprising, helical cylinders do not form readily because

it requires energy to bend the cylinders. Multiple helices were probably favored in this case due to the marginal solubility of the PBMA chains and the right relative length between the PtBA and PBMA blocks. With their marginal solubility, PBMA chains of different cylinders would like to associate. Extensive association could lead to the clustering of many cylinders per bundle and thus the precipitation of the polymer. This was prevented because the PtBA chains were soluble and the PBMA chains were not totally insoluble. An optimal PtBA/PBMA chain-length ratio was deemed important because too short a PtBA block would have failed in preventing polymer precipitation, whereas too long a PtBA block would have prevented the PBMA chains of different cylinders from contacting one another. The cylinders clustered and twisted into multiple helices because it helped increase PBMA chain mixing and decrease PBMA/solvent contact.

How double-helix formation helped to reduce PBMA/solvent contact is best seen in Figure 4b, which shows the twisting of a green and a red pipe cleaner into a double helix. The metal-wire core here would be the analogue of the PCEMA core of the triblock-copolymer cylindrical aggregates. The green and red bristles can be viewed as the coronal PBMA chains. (There is no PtBA chain equivalent in this analogy unless we dye some of the green and red bristles into a different color.) Obviously, there is more bristle and air contact (PBMA and solvent contact) in the section in which the pipe cleaners are not twisted.

Although helical-cylindrical-domain formation from one block of a copolymer has been observed in block-segregated copolymer solids,^[26,27] we believe that this is the first report on the formation of multiple helices as the major product from block-copolymer solution self-assembly. Nolte and co-workers^[28] reported the formation of a helical-cylindrical superstructure from the self-assembly of an AB diblock copolymer containing a chiral peptide block. The structural details, for example, the polymer-chain packing in such a single-helix superstructure, were unknown. Geng et al.^[29] observed, by fluorescence microscopy, single cylinders with irregularly twisted helical sections from an AB diblock copolymer with one block again containing chiral peptide units. A correlation between the cylinder and copolymer structures was not made. The twisting of single cylinders in these two cases was not surprising and was attributed to the oriented packing of the chiral blocks in the cylindrical cores. Helical aggregates have also been observed from ill-defined multiple-block copolymers containing helical poly(methylphenylsilane) blocks.^[30] The co-twisting of two helical poly(methylphenylsilane)-chain bundles was hypothesized to lead to the final superhelical aggregates. Liu and co-workers^[31] recently reported on the formation of single cylinders with twisted sections from ABC achiral triblock copolymers; Pochan, Wooley, and co-workers^[32] reported on the formation of helices with regular pitches. The single cylinders twisted in the former case because of coronal A and C chain segregation and surface repulsive-force asymmetry. In the latter case, the major products were single rather than double helices. These strands had poly(acrylic acid) chains on their surfaces. The interaction between multiamines and poly(acrylic acid) chains was

thought to provide the buckling force to bend the cylinders into helices.

In summary, PBMA₃₅₀-*b*-PCEMA₁₆₀-*b*-PtBA₁₅₀ has been self-assembled in three solvent mixtures. These solvents were good for the PtBA block, poor for the PCEMA block, and marginal for the PBMA block. After long periods, double helices and occasional triple helices were the self-assembled products. The generality of such conditions for helix formation remains to be established.

Experimental Section

For helix preparation, the triblock copolymer was first dissolved in CH₂Cl₂, CHCl₃, or C₄H₈O at 5 mg mL⁻¹. MeOH was then added within 1 min to the solution in a vial under vigorous stirring until the desired *f_M* value was reached. The vial was sealed and placed in a closed desiccator containing a small amount of the same solvent mixture at the bottom to minimize evaporation-induced solvent-composition change inside the vial. During aging, all samples were magnetically stirred.

For TEM, aggregates were sprayed onto carbon-coated copper grids and stained by OsO₄ vapor for 2 h. All TEM observations were made on a Hitachi 7000 instrument operated at 75 kV.

For electron tomography, a 10 nm Au colloidal solution (GCN005, BBInternational Ltd., UK) was placed on a TEM grid containing the helices. TEM tomography analysis was done by using a JEM-2200FS (JEOL Co. Ltd., Japan) instrument operated at 200 kV. Only the transmitted and elastically scattered electrons with energy loss between 0 and ±15 eV were used for imaging. The images or projections were collected at sample-tilting angles ranging from -71° to 77° at 1° intervals. The series of images were aligned by the fiducial marker method^[33] by using the Au particles. The 3D images were reconstructed based on the filtered back projection method.^[34]

Received: March 19, 2009

Published online: July 7, 2009

Keywords: block copolymers · helical structures · micelles · nanostructures · self-assembly

- [1] M. Lazzari, G. J. Liu, S. Lecommandoux, *Block Copolymers in Nanoscience*, Wiley-VCH, Weinheim, **2006**.
- [2] L. F. Zhang, A. Eisenberg, *Science* **1995**, *268*, 1728–1731.
- [3] J. F. Ding, G. J. Liu, M. L. Yang, *Polymer* **1997**, *38*, 5497–5501.
- [4] J. F. Ding, G. J. Liu, *Macromolecules* **1997**, *30*, 655–657.
- [5] D. E. Discher, A. Eisenberg, *Science* **2002**, *297*, 967–973.
- [6] G. J. Liu, *Adv. Polym. Sci.* **2008**, *220*, 29–64.
- [7] J. Ruez, I. Manners, M. A. Winnik, *J. Am. Chem. Soc.* **2002**, *124*, 10381–10395.
- [8] G. Njikang, D. H. Han, J. Wang, G. J. Liu, *Macromolecules* **2008**, *41*, 9727–9735.
- [9] C. Price, *Pure Appl. Chem.* **1983**, *55*, 1563–1572.
- [10] J. Tao, S. Stewart, G. J. Liu, M. L. Yang, *Macromolecules* **1997**, *30*, 2738–2745.
- [11] S. Jain, F. S. Bates, *Science* **2003**, *300*, 460–464.
- [12] Z. Y. Chen, H. G. Cui, K. Hales, Z. B. Li, K. Qi, D. J. Pochan, K. L. Wooley, *J. Am. Chem. Soc.* **2005**, *127*, 8592–8593.
- [13] D. J. Pochan, Z. Y. Chen, H. G. Cui, K. Hales, K. Qi, K. L. Wooley, *Science* **2004**, *306*, 94–97.
- [14] Z. B. Li, E. Kesselman, Y. Talmon, M. A. Hillmyer, T. P. Lodge, *Science* **2004**, *306*, 98–101.
- [15] X. S. Wang, G. Guerin, H. Wang, Y. S. Wang, I. Manners, M. A. Winnik, *Science* **2007**, *317*, 644–647.
- [16] N. Hadjichristidis, H. Iatrou, M. Pitsikalis, S. Pispas, A. Avgeropoulos, *Prog. Polym. Sci.* **2005**, *30*, 725–782.
- [17] C. A. Fustin, V. Abetz, J. F. Gohy, *Eur. Phys. J. E* **2005**, *16*, 291–302.
- [18] K. Hales, Z. Y. Chen, K. L. Wooley, D. J. Pochan, *Nano Lett.* **2008**, *8*, 2023–2026.
- [19] T. P. Lodge, J. Bang, Z. B. Li, M. A. Hillmyer, Y. Talmon, *Faraday Discuss.* **2005**, *128*, 1–12.
- [20] J. T. Zhu, W. Jiang, *Macromolecules* **2005**, *38*, 9315–9323.
- [21] M. Schmalz, J. Schmelz, M. Drechsler, J. Yuan, A. Walther, K. Schweimer, A. M. Mihut, *Macromolecules* **2008**, *41*, 3235–3242.
- [22] H. V. Berlepsch, C. Bottcher, K. Skrabania, A. Laschewsky, *Chem. Commun.* **2009**, 2290–2292.
- [23] E. Hoppenbrouwers, Z. Li, G. J. Liu, *Macromolecules* **2003**, *36*, 876–881.
- [24] F. T. Liu, A. Eisenberg, *J. Am. Chem. Soc.* **2003**, *125*, 15059–15064.
- [25] J. Israelachvili, *Intermolecular & Surface Forces*, Academic Press, London, **1992**.
- [26] H. Jinnai, T. Kaneko, K. Matsunaga, C. Abetz, V. Abetz, *Soft Matter* **2009**, *5*, 2042–2046.
- [27] H. Xiang, K. Shin, T. Kim, S. I. Moon, T. J. McCarthy, T. P. Russell, *Macromolecules* **2005**, *38*, 1055–1056.
- [28] J. Cornelissen, M. Fischer, N. Sommerdijk, R. J. M. Nolte, *Science* **1998**, *280*, 1427–1430.
- [29] Y. Geng, D. E. Discher, J. Justynska, H. Schlaad, *Angew. Chem.* **2006**, *118*, 7740–7743; *Angew. Chem. Int. Ed.* **2006**, *45*, 7578–7581.
- [30] N. A. J. M. Sommerdijk, S. J. Holder, R. C. Hiorns, R. G. Jones, R. J. M. Nolte, *Macromolecules* **2000**, *33*, 8289–8294.
- [31] J. W. Hu, G. Njikang, G. J. Liu, *Macromolecules* **2008**, *41*, 7993–7999.
- [32] S. Zhong, H. G. Cui, Z. Y. Chen, K. L. Wooley, D. J. Pochan, *Soft Matter* **2008**, *4*, 90–93.
- [33] R. A. Crowther, D. J. Derosier, A. Klug, *Proc. R. Soc. London Ser. A* **1970**, *317*, 319–340.
- [34] H. Jinnai, R. J. Spontak, *Polymer* **2009**, *50*, 1067–1087.